Melt-dominated mid-crust in the 575–500 Ma Damara Orogen: Field constraints on an interconnected migmatite–granite system

Thomas L. Jones[1,2*], A. Otto[3], E. Becker[3,4] and Andy Wilde[5]

Corresponding author: tl.jonesy8@gmail.com

[1]*School of Geosciences, University of the Witwatersrand, Johannesburg, South Africa.*

[2]*TLJ Structural Geology Consulting Ltd, Edinburgh, United Kingdom*

[3]*Deep Yellow Ltd, Subiaco, Western Australia*

[4]*Marc Geology Pty Ltd, Hillarys, Western Australia*

[5]*Boss Energy, 1/420 Hay Street, Subiaco, WA 6010, Western Australia*

Keywords: Migmatite, leucogranite, high-temperature metamorphism, partial melting, rheology, orogen

ABSTRACT

Modern thermomechanical models emphasise the role of partial melting and granite magmatism on the structural and tectonic evolution of orogenic belts. Partially molten mid-crust can trigger a change from localised deformation to distributed ductile flow, while also accommodating chemical differentiation of the crust. In the southern Central Zone of Namibia's Damara Orogen, it is unclear whether high-temperature granulite-facies rocks consisted of relatively isolated zones of crustal melting within a predominantly rigid crust, or contained sufficiently widespread partially molten rocks such as to be capable of modifying mechanical behaviour during deformation. Here, we use extensive cross-cutting field relationships, remote sensing, and whole-rock geochemistry to investigate the composition, physical state, and magmatic architecture in the cores of two dome structures. The outcrop area is dominated by metatexite and diatexite migmatites, larger interconnected leucogranite dyke networks and pluton-like accumulations, and subordinate entrained metasedimentary rafts and schlieren. Migmatites and leucogranites intrude into and cross-cut the overlying ca. 870-590 Ma Damara Supergroup along a diffuse and intrusive contact. Geochemical data records similar major, trace, and REE-element patterns between leucosomes in the underlying migmatites and leucogranite dykes intruding into the overlying Damara Supergroup. Overlying leucogranite dykes are more evolved than underlying leucosomes, consistent with differentiation during magma extraction and ascent. Partially molten crust therefore formed a volumetrically dominant interconnected domain throughout deeper structural levels in the cores of these dome structures, providing a foundation for broader discussion on deformation mechanisms and the potential for distributed ductile flow in the Damaran mid-crust.

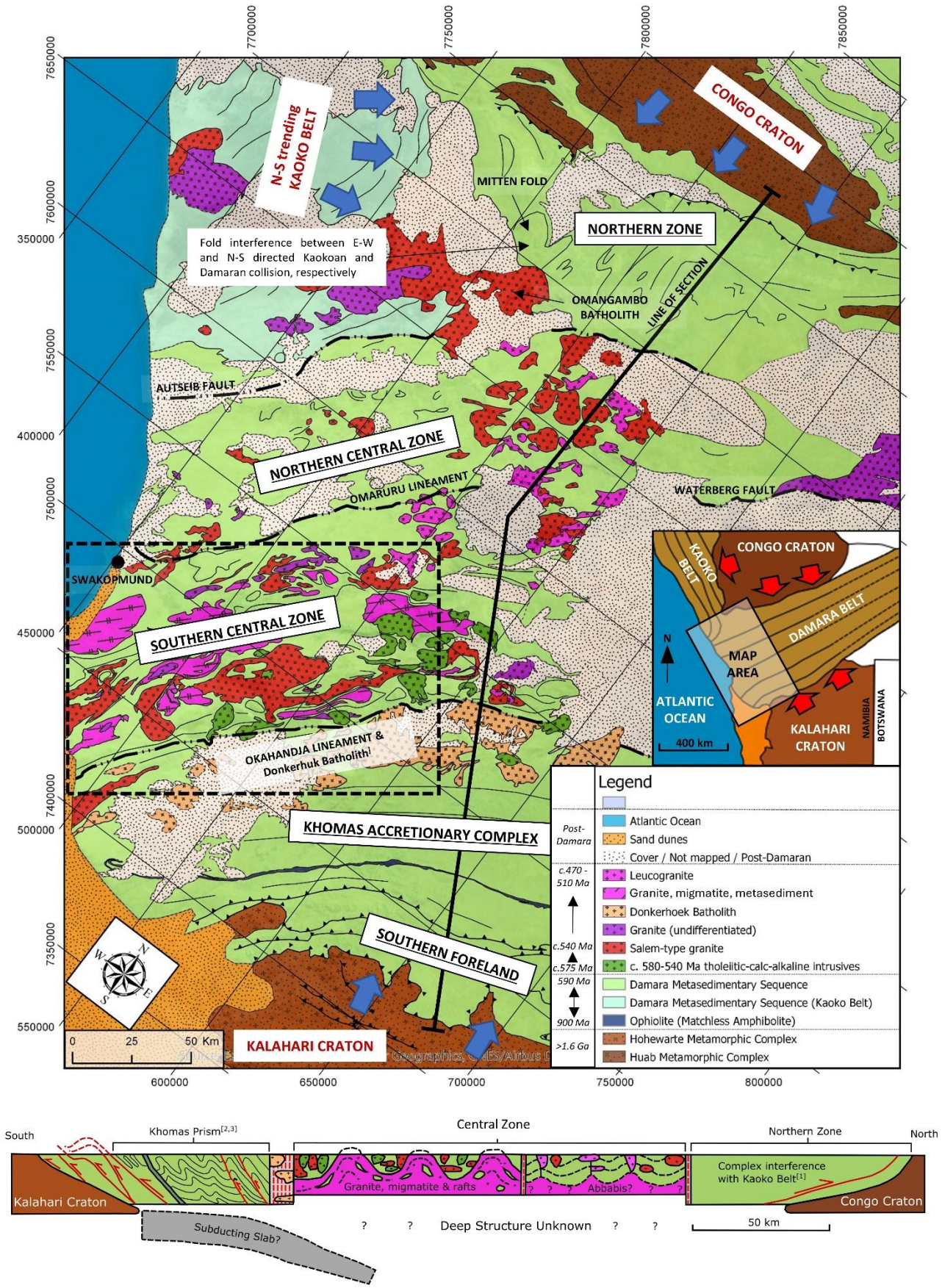

Figure 1 – Regional geological map and interpretative cross-section of the Damara Orogen, modified after Miller and Grote (1988), Geological Survey of Namibia (Sheets 2214, 2216, 2116, 2114, 2014), and Knupp (2019).

1. INTRODUCTION

Partially molten mid-crustal domains strongly influence the rheology, deformation style, and tectonic evolution of collisional orogens. Modest melt fractions below 10% are sufficient to cause a 90% decrease in the strength of rocks measured in the laboratory; this strength reduction is attributed to the development of interconnected melt films along grain boundaries which cause a transition from intracrystalline deformation to melt-lubricated intergranular deformation (Rosenberg and Handy, 2005). Small volumes of melt reduce effective viscosity and substantially weaken the crust (Jamieson et al., 2011). If melt is present over wider areas, this can promote a transition from localised strain accumulation to distributed ductile flow of the mid-crust. The transition from melt-absent to melt-present deformation has fundamental implications for the style and tectonic evolution of orogenic belts (Jamieson and Beaumont, 2013).

In the southern Central Zone of the Damara Orogen in Namibia, the origin of complex dome-and-basin structures and heterogeneous fold interference patterns has been discussed and debated for decades, with no consensus on their mechanism of formation (e.g., Barnes and Downing, 1979; Jacob et al., 1983; Kroner, 1984; Oliver, 1994, 1995; Poli and Oliver, 2001; Kisters et al., 2004; Ormond et al., 2024). These structures developed contemporaneously with granulite-facies metamorphism, partial melting, and leucogranite magmatism at ca. 530–510 Ma. While the presence of crustal melting is recognised, the extent and structural significance of partially molten crust within the southern Central Zone remain inadequately constrained. The extent of Damaran magmatism at deeper structural levels in the cores of km-scale dome structures – including amongst an older pre-Damaran basement block termed the Abbabis Complex – is particularly unclear. It is therefore uncertain whether the southern Central Zone preserves relatively isolated zones of crustal melting within a predominantly rigid crust, or consists of sufficiently widespread partially molten mid-crust capable of modifying mechanical behavior during deformation.

In this study, we use detailed structural field observations and rigorous analysis of cross-cutting relationships, supported by remote sensing observations and whole-rock geochemistry, to study the composition, physical state, and magmatic architecture in two of the best-exposed dome structures along the lower Swakop River section of the southern Central Zone. We investigate the hypothesis that the deepest exposed structural levels of the southern Central Zone contain a more extensive Damaran-aged migmatite–granite system than is currently recognised on existing maps. This study concerns the composition and physical state of the exhumed mid-crust, providing the geological basis for a broader

discussion of deformation mechanisms and tectonic evolution in related companion studies (Jones, 2026; Jones et al., 2026).

GEOLOGICAL SETTING

The Damara Belt records northwest-southeast convergence between the Congo and Kalahari cratons at c. 575-500 Ma during the assembly of the supercontinent Gondwana. The Damara Belt consists of oppositely verging wedges of the Northern and Southern zones bookending km-scale domes and fold interference structures in the Central Zone (Figure 1). During collision, the Northern and Southern zones were metamorphosed at relatively low-T and high-P conditions of 8-9 kbar and 10 kbar, respectively (Goscombe et al., 2017), while rocks in the Central Zone underwent higher-temperature / lower-pressure metamorphism.

The southern Central Zone records the highest metamorphic temperatures in the orogen, with regional metamorphic conditions of ~800^{O}C at pressures of 4-5 kbar occurring at c. 520 Ma (Longridge et al., 2017; Jung et al., 2019). This high-temperature metamorphic event triggered in-situ partial melting of metasedimentary units, leading to the formation of large volumes of leucogranites in the Central Zone (e.g., Ward et al., 2008; Kisters et al., 2009; Jung et al., 2019). Leucogranites mostly have S-type signatures (Jung et al., 2001; Paul et al., 2014), although some also have slight I-type signatures (Ashworth et al., 2020).

The stratigraphy of the southern Central Zone is reported to consist of a Neoproterozoic Damara Metasedimentary Supergroup deposited unconformably onto Palaeoproterozoic-Mesoproterozoic Abbabis Complex basement. The lower Nosib Group of the Damara Supergroup reportedly consists of quartzites of the Etusis Formation overlain by diopside-feldspar gneiss, biotite schist and cordierite gneiss of the Khan Formation. The upper Swakop Group consists of distinctive marble-bearing sequences of the Rossing Formation, overlain by diamictite and meta-ironstone of the Chuos Formation, as well as marble of the Arandis Formation. These are overlain by thick marble and dolomite units of the Karibib Formation, as well as a thick package of pelitic schists attributed to an uppermost Kuiseb Formation (Smith, 1965; Jacob, 1974; Hoffmann et al., 2004; Miller, 2008).

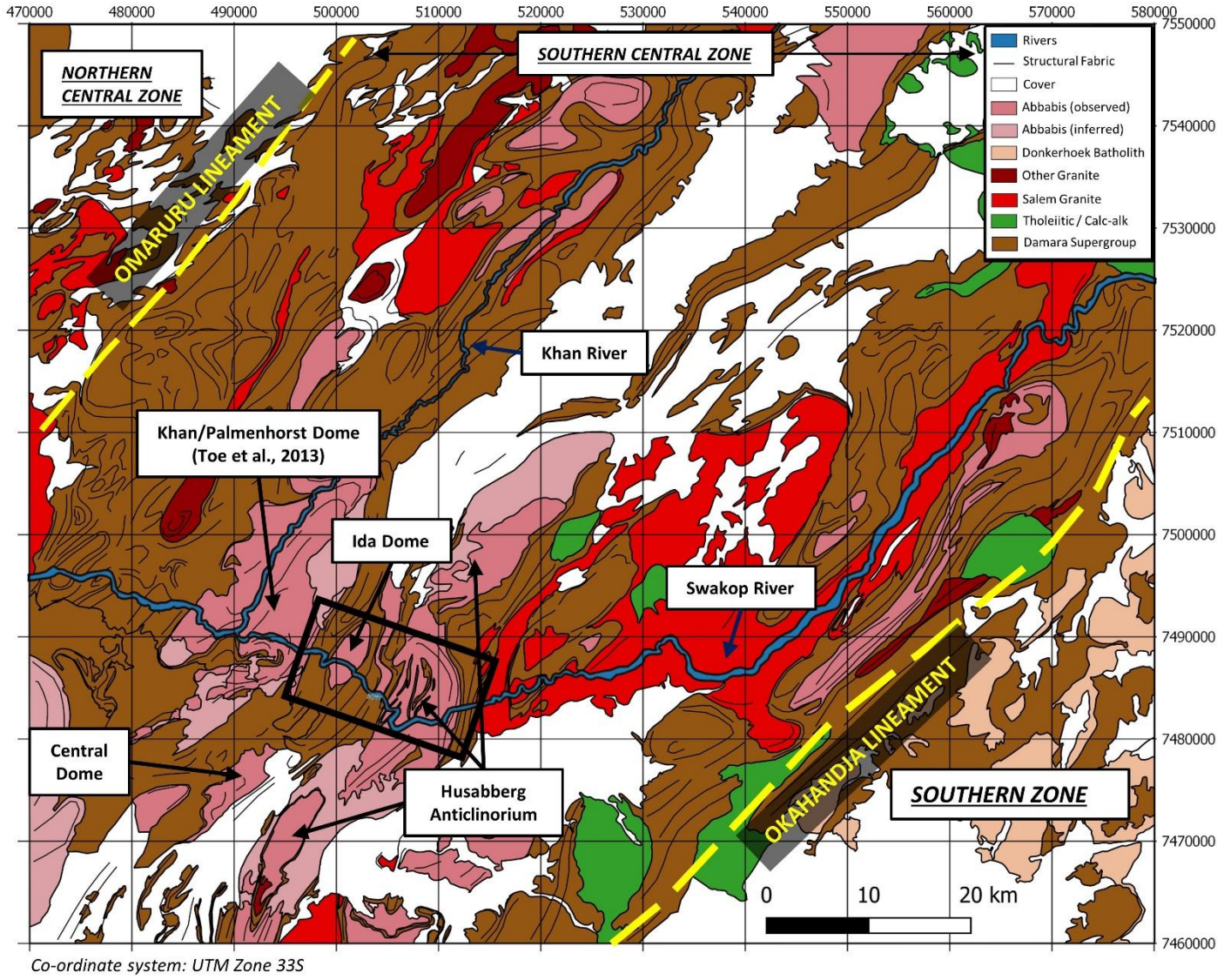

Figure 2 – Simplified geological map of the southern Central Zone in the vicinity of the Khan and Swakop rivers (modified after Geological Survey of Namibia Sheet 2214 and Knupp, 2019). Black box along the lower Swakop River outlines the study area in the Ida Dome and Husabberg Anticlinorium.

2. DATASETS & METHODOLOGY

New field mapping was undertaken across two km-scale dome structures termed the Ida Dome and Husabberg Anticlinorium (Figure 2). The Swakop River provided near 100% outcrop exposure through both dome structures. Field observations were supplemented with an interpretation of airborne radiometric, magnetic, and hyperspectral data (Figure 3) to create a detailed new lithological map of the study area (Figure 4). The locations of key features and field photos (Figure 5 to 12) are shown on the geological map in Figure 4. Key observations are annotated on the schematic cross-section in Figure 4. Twenty samples were collected for geochemical analysis, with their location shown in Figure 4. Eight samples of granitic leucosome were collected from migmatites in the core of the Ida Dome, as well as 12 samples of leucogranite dykes intruding into the overlying Damara Supergroup on the dome limbs (Figure 4). Samples were submitted to ALS Laboratories in Okahandja, Namibia, for analysis in Perth, Western Australia. Samples were crushed and pulverized to 85% passing 75 µm. Major element oxides were determined using the ALS ME-ICP06 whole-rock package following lithium borate fusion, with concentrations measured by inductively coupled plasma–atomic emission spectrometry (ICP-AES). Trace elements were analysed using lithium borate fusion with inductively coupled plasma–mass spectrometry (ICP-MS; method ME-MS81). Loss on ignition (LOI) was determined by thermogravimetric analysis (TGA furnace; method ME-GRA05). Selected base metals were analysed following four-acid digestion (ME-4ACD81). Analytical precision and accuracy were monitored using internal standards and quality control procedures implemented by ALS.

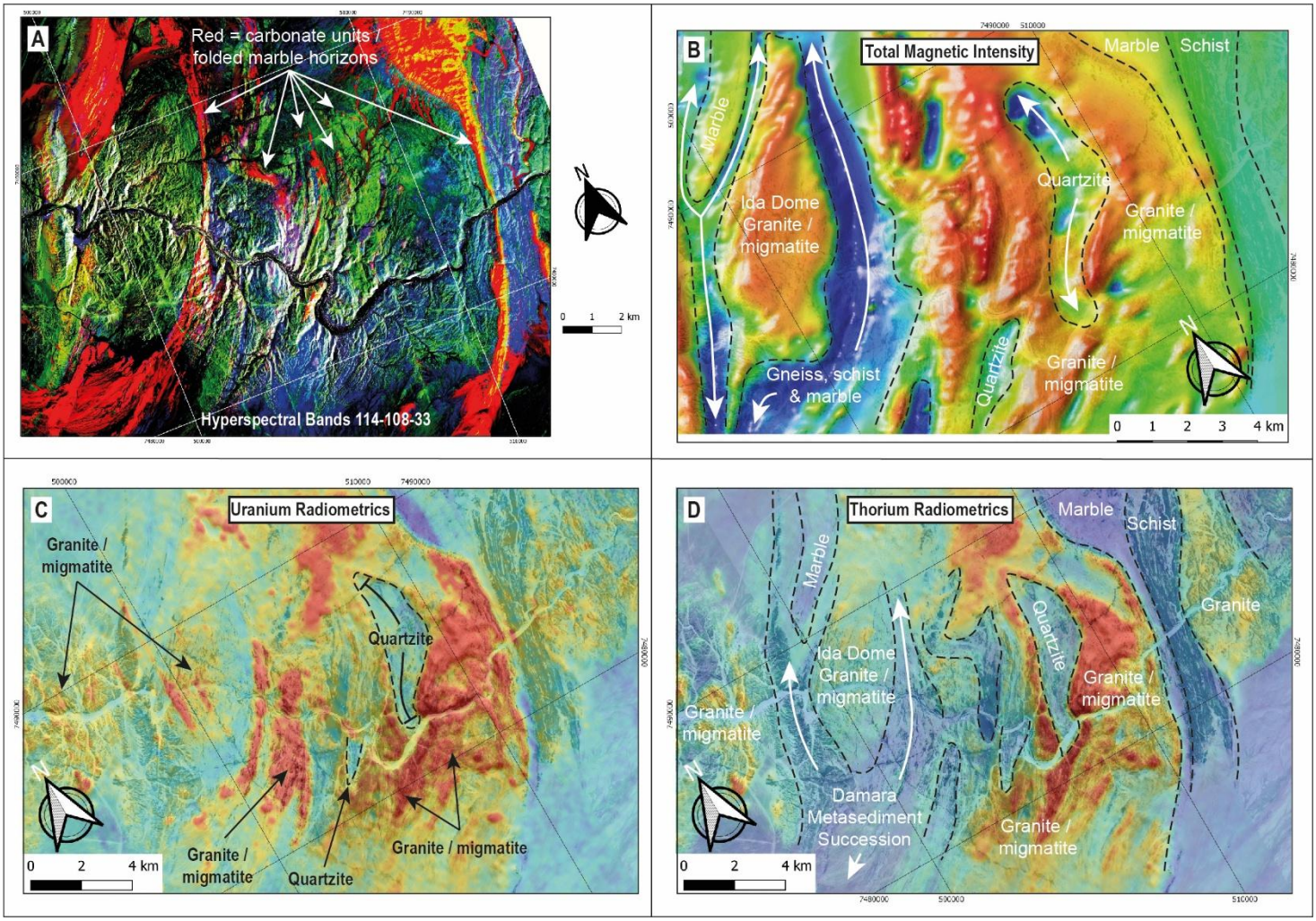

Figure 3 – Example remote sensing datasets used to delineate different metasedimentary rock units amongst granites and migmatites along the lower Swakop River. A) Hyperspectral image of bands 114-108-33. B) Total Magnetic Intensity Reduced to Pole. C) Uranium distribution. D) Thorium distribution.

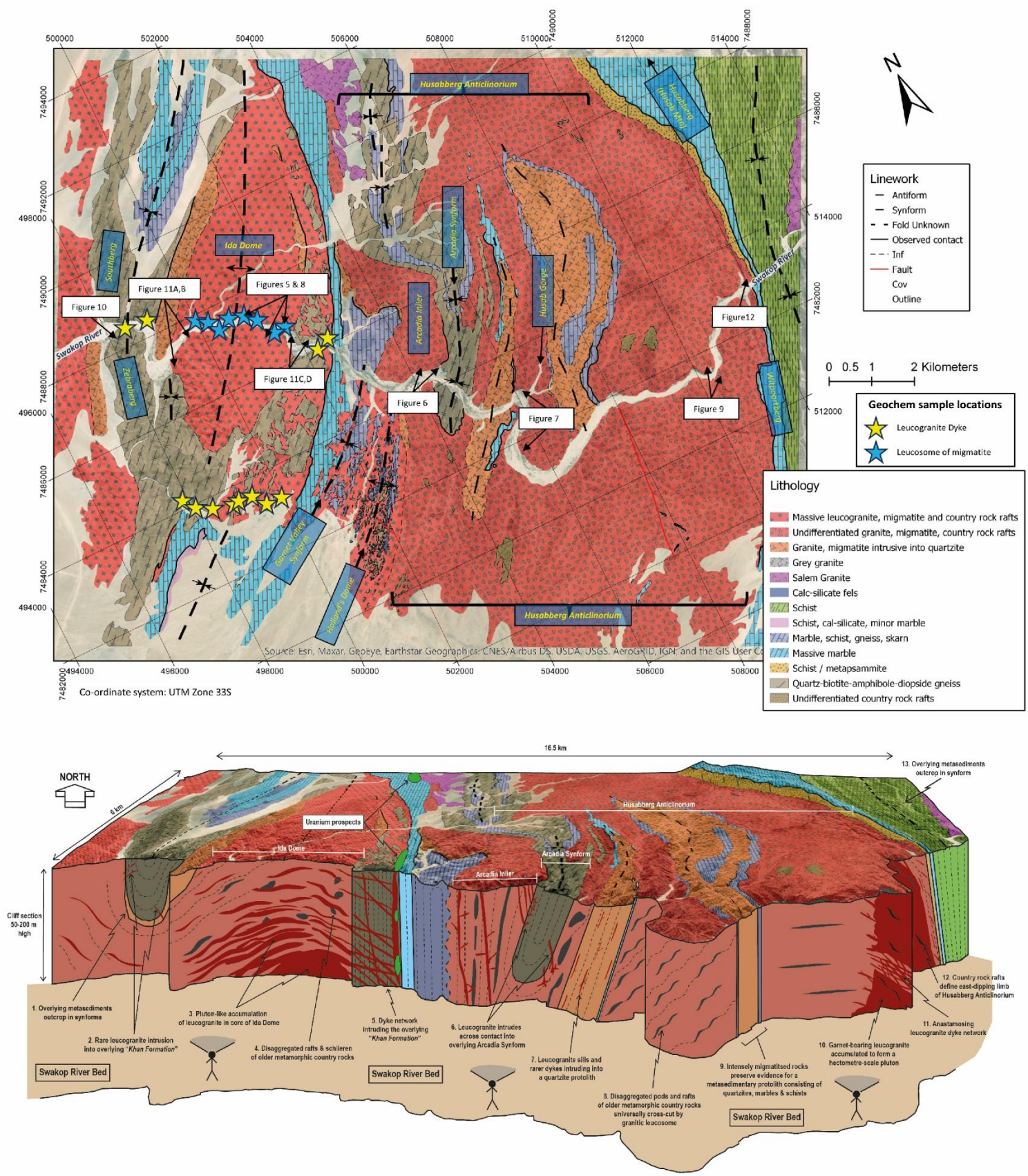

Figure 4 – Geological map and schematic cross-section of the study area illustrating key field relationships. Location of field photos and samples collected for geochemical analysis are shown on the map.

3. RESULTS

3.1 Migmatites and granites in the core of the Ida Dome and Husabberg Anticlinorium

Three principal rock units dominate the outcrop area in the core of the Ida Dome and Husabberg Anticlinorium: i) metatexite and diatexite migmatites, ii) larger leucogranite, dykes, sills and plutons, and iii) rafts, schlieren, and occasional laterally continuous horizons of metasedimentary rocks.

3.1.1 Metatexite & diatexite migmatites & evidence for petrographic continuity

Metatexite and diatexite migmatites dominate the outcrop area in both domes (Figures 5-7). At the Ida Dome, the proportion of granite increases with depth; metatexite migmatites grade into diatexite migmatites at deeper structural levels (Figure 4). Migmatites show typical patch, stromatic, and net-like textures (Figure 5A-C). Petrographic continuity is common; stromatic leucosomes merge with leucosome bodies in discordant shear bands (Figure 5C) and dyke-like structures (Figure 5D). At the Arcadia Inlier (location shown in Figure 4), petrographic continuity is well-developed between foliation-parallel pinch-and-swell leucosomes and larger discordant leucogranite dykes (Figure 6B-C). In the Husabberg Ancticlinorium**,** diffuse patch migmatites are locally associated with distinctive garnet megacrysts (Figure 7A); stromatic leucosomes lead away from the patch migmatites and feed into larger leucogranite dykes which transgress the foliation (Figure 7B). Diatexite migmatites form km-thick rock bodies which dominate the outcrop area east of the Husab Gorge (Figure 4 and 7). The bulk of granitic leucosome is arranged as thin bodies oriented parallel to the foliation in the country rock gneisses. Similar field relations were observed throughout the approximately 16 km wide transect through the cores of both dome structures; this attests to an areally and volumetrically extensive migmatite complex (Figure 3-7).

23

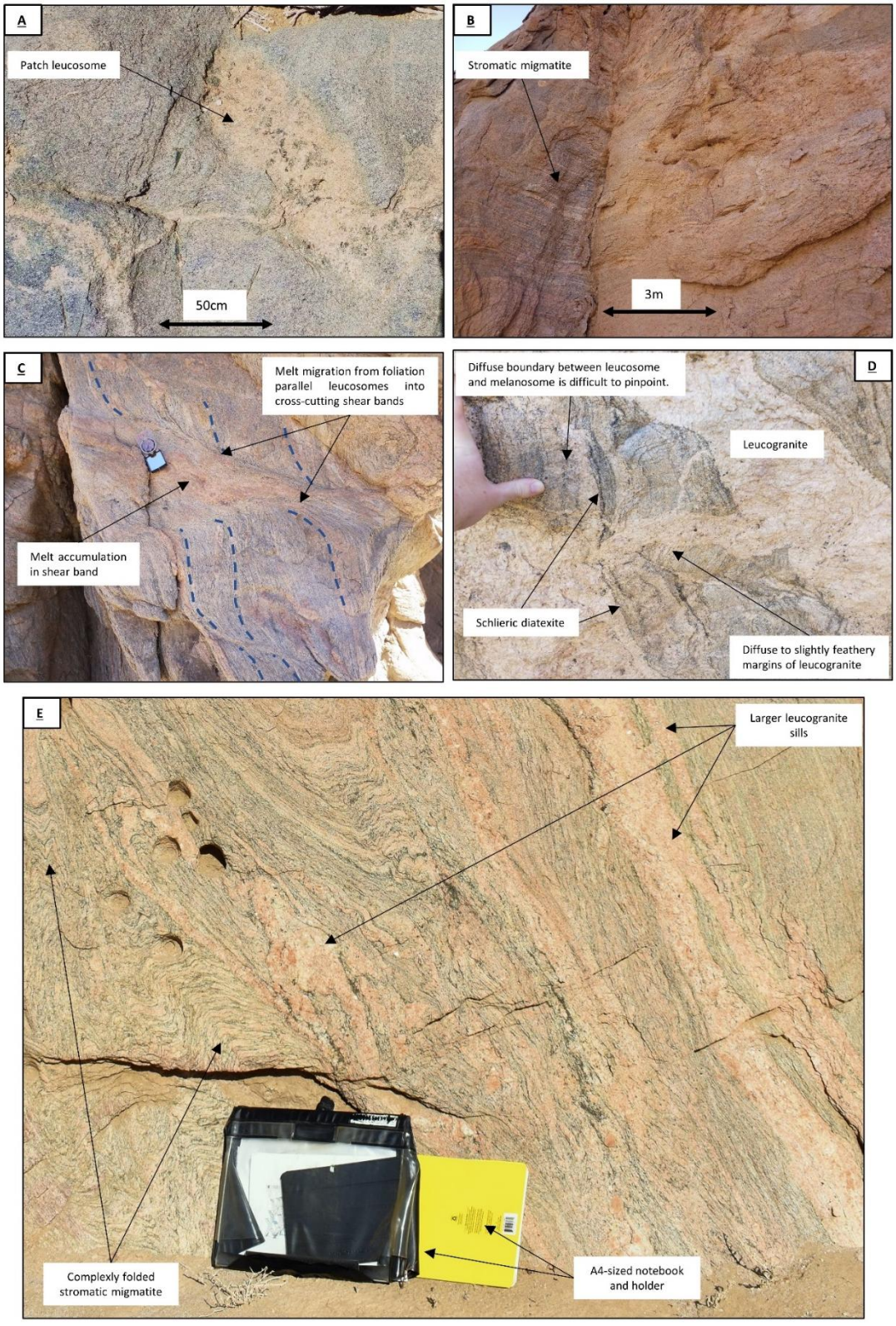

Figure 5 – Migmatites in the core of the Ida Dome. A) Patch migmatite; B) Stromatic migmatite; C) Net-textured migmatite D) Cross-cutting dyke-like structure with locally diffuse & feathery margins; E) Complex migmatite outcrop patterns .

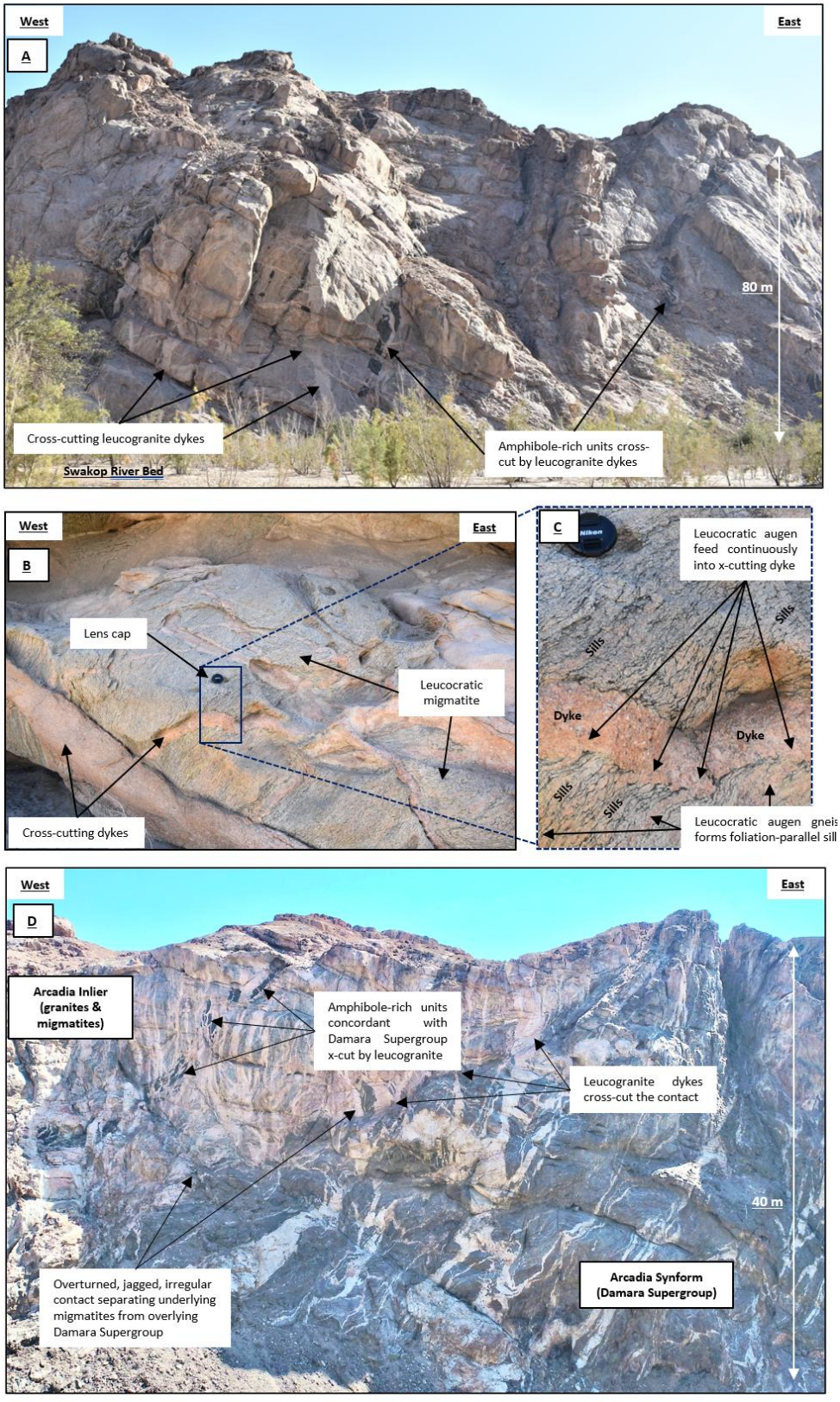

Figure 6 – Migmatites and granites at the Arcadia Inlier. A) Migmatites and amphibole-rich units transgressed by leucogranite dykes. B) Close-up of [A]. C) Close up of [B] showing petrographic continuity between leucosomes and larger dyke-like structures. D) Overturned contact between underlying migmatites and the "Khan Formation" of the Damara Supergroup – note the absence of the "Etusis Formation", as well as leucogranite dykes intruding across the contact and into the metasediments of the Damara Supergroup.

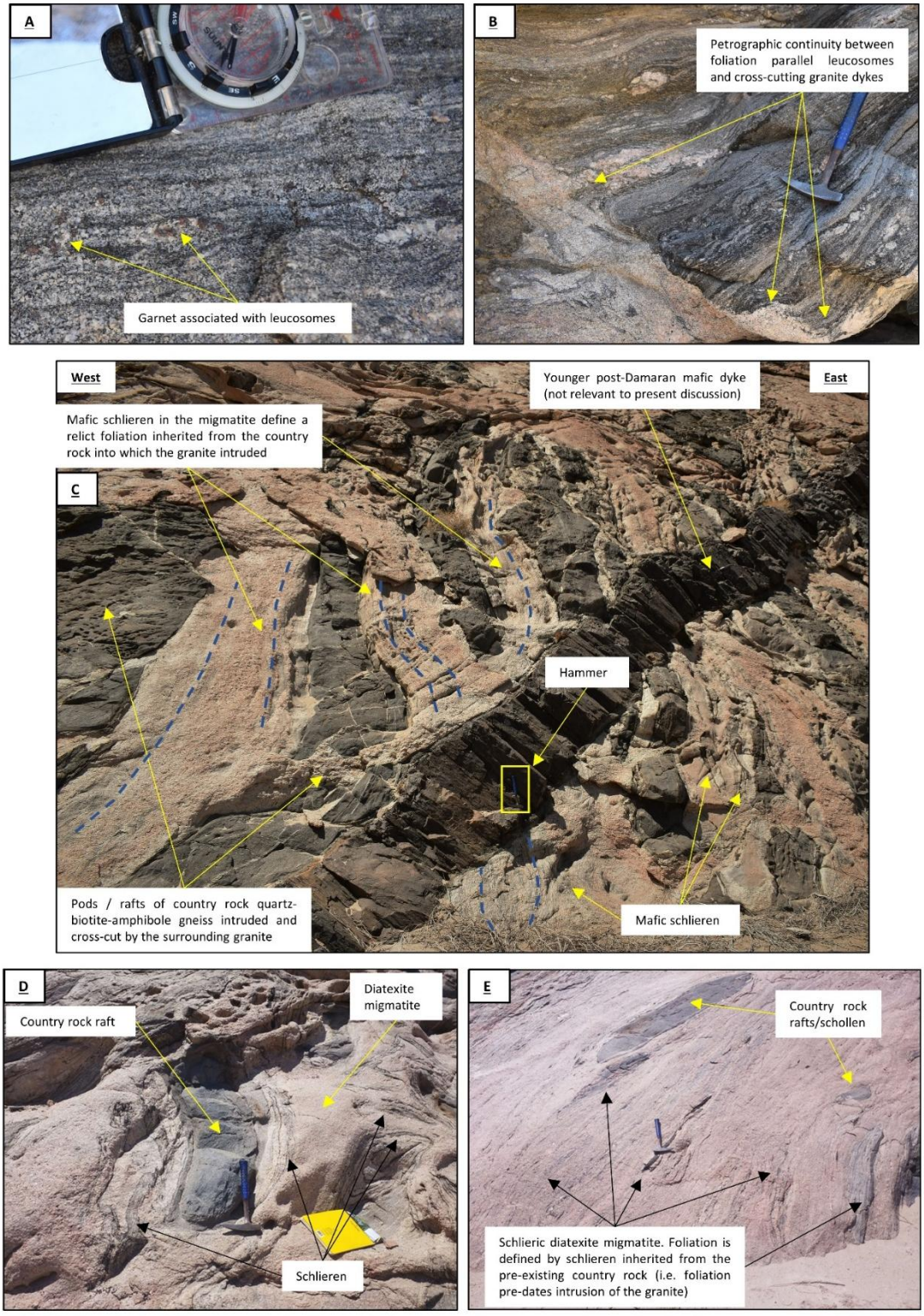

Figure 7 – Migmatites in the core of the Husabberg Anticlinorium, outcropping west and east of the Husab Gorge. A) Garnet crystals associated with granitic leucosome; B) Foliation-parallel leucosomes show petrographic continuity with larger cross-cutting leucogranite dykes; C, D & E) Schollen and schlieric diatexite migmatites preserving rafts of quartz-biotite-amphibole gneiss.

25

26

3.1.2 Larger leucogranite dykes, sills, and plutons

Larger leucogranite dykes, sills and plutons show petrographic continuity with leucosomes in the migmatites. The proportion of leucogranite rises from 40-60 % on the western limb of the Ida Dome to >80 % massive leucogranite at the deepest structural level in the dome core (Figure 8). The core of the Ida Dome constitutes a pluton-like accumulation of leucogranite (Figure 4 & 8). At the Husabberg Anticlinorium, another pluton-like accumulation of leucogranite outcrops towards the eastern edge of the dome (Figure 4 & 9A). This pluton is several hundred metres thick. It consists of an anastomosing network of leucogranite dykes (Figure 9B), as well as cm-thick leucogranite sills arranged along foliation planes (Figure 9D). Leucogranite dykes and sills merge seamlessly with each other and do not sharply cross-cut one another (Figure 9). The granitic component consistently cross-cuts metamorphic fabrics in both of these pluton-like bodies (Figure 8 and 9).

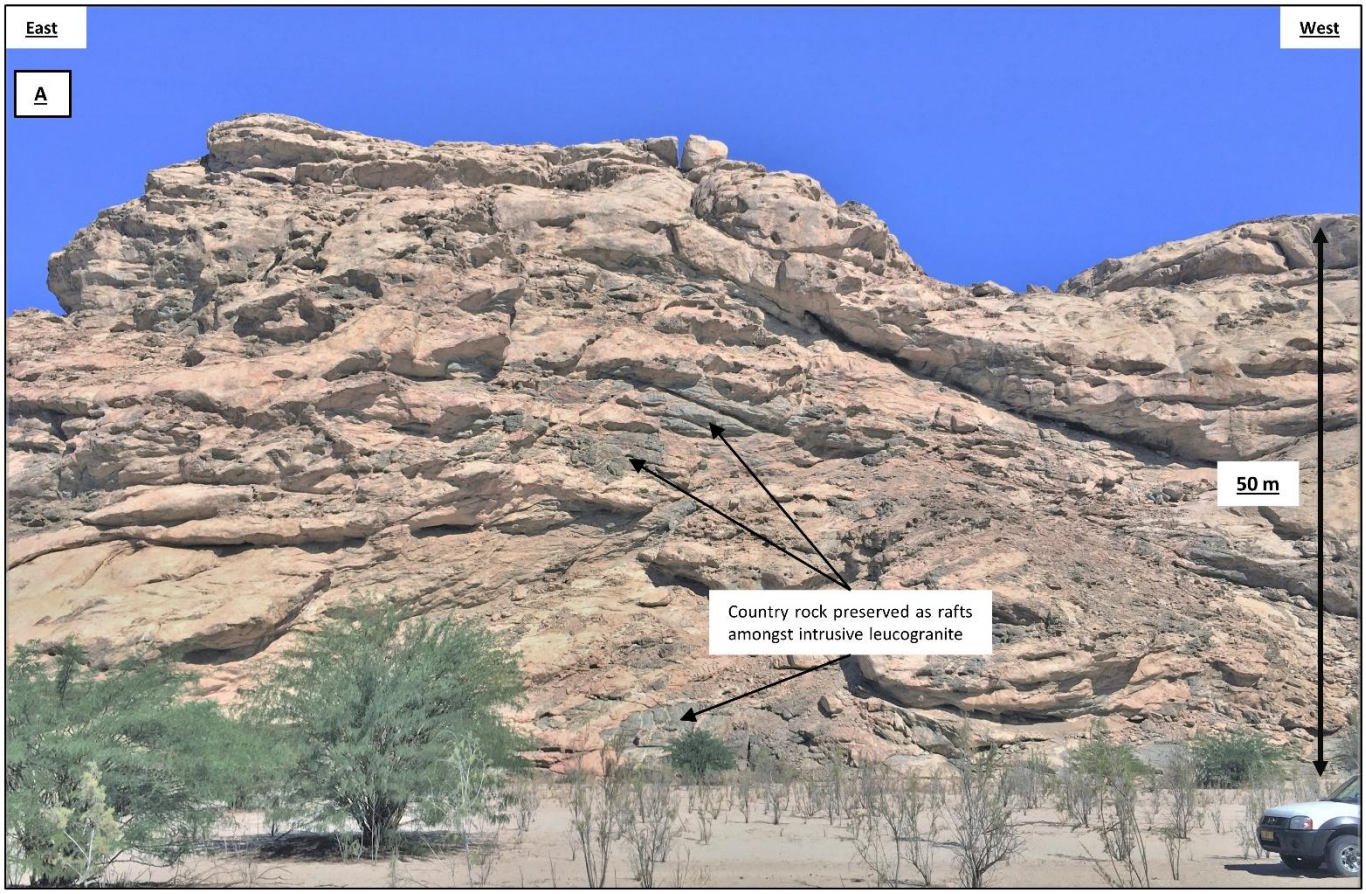

Figure 8 – Pluton-like accumulation of leucogranite / diatexite migmatite at the deepest exposed level in the core of the Ida Dome.

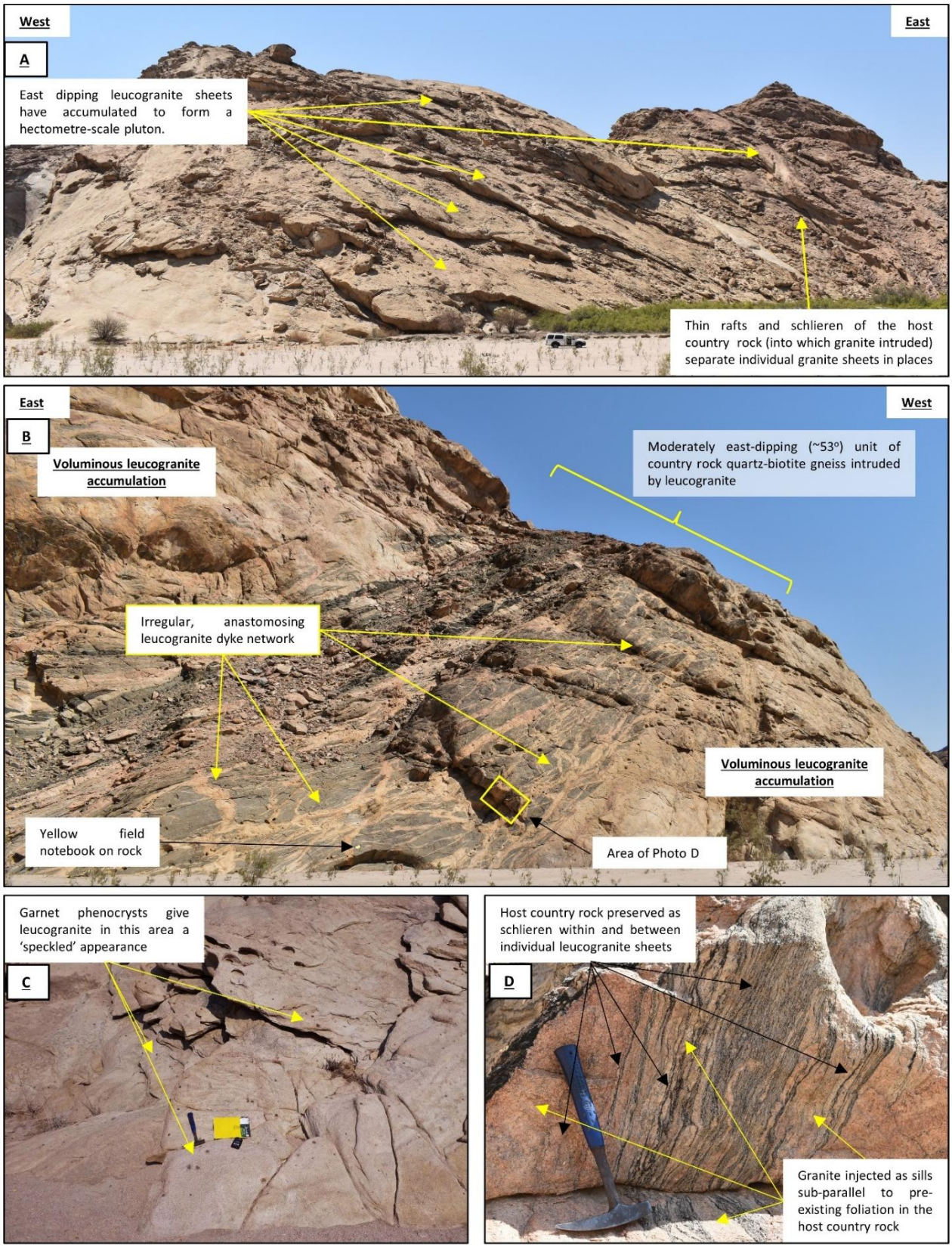

Figure 9 – Pluton-like accumulation of leucogranite near the eastern edge of the Husabberg Anticlinorium. A) Leucogranite pluton formed from the accumulation of individual east-dipping leucogranite sheets. B) Anastomosing leucogranite dykes. C) Garnet phenocrysts. D) Close-up of (B) showing the intrusion of numerous small leucogranite sills oriented sub-parallel to the foliation planes, giving the rock an overall lit-par-lit appearance.

3.1.3 Rafts, schlieren and laterally continuous metasedimentary horizons

Older metamorphic country rock protoliths are preserved as rafts, schlieren, and laterally continuous horizons amongst the migmatites. They are cross-cut by the surrounding migmatites and leucogranites (Figures 6 to 9). Country rock rafts and schlieren are compositionally diverse; quartz-biotite+/-amphibole gneisses are common and typically show concordant fabrics with surrounding stromatic leucosomes (Figure 6 and 7). Locally, the rafts are sheared and rotated by the surrounding granite. More massive quartzite units, containing heavy mineral laminae of magnetite and ilmenite locally arranged in structures resembling cross-bedding, are observed as 20-30 metre-thick bodies amongst migmatites in the core of the Ida Dome. A massive quartzite unit dominates core of the Husabberg Anticlinorium (Figure 4) and is distinctive on airborne magnetic and radiometric data (Figure 3). Carbonate-bearing sequences are distinguished on hyperspectral datasets and form thin but laterally-continuous folded horizons in the core of the Husabberg Anticlinorium (Figure 3A and 4; as also mapped by Barnes, 1981). These carbonate sequences outcrop as a 100 metre thick unit of mottled diopside-garnet-epidote-gneiss, plus 10-14 m thick package of marbles and schists, along the Swakop River. Marble units and quartzites attest to a significant metasedimentary component in the country rock protoliths to the migmatites throughout the study area.

3.2 Field geology of the overlying Damara Metasedimentary Supergroup

Metasedimentary units closely match the accepted stratigraphic succession of the Neoproterozoic Damara Supergroup on the limbs of the Ida Dome. They consist of (1) quartzites and meta-sandstones (*Etusis Formation*); (2) an overlying, well-developed, several hundred metres thick sequence of quartz-diopside-epidote-amphibole-biotite gneiss (*Khan Formation*; Figure 10), and (3) marble units (*Rössing Formation*).

The Arcadia Synform exposes the "*Khan*" and "*Rössing*" formations of the Damara Supergroup (Barnes, 1981; Longridge, 2012; Kruger and Kisters, 2016). The *Khan Formation* here is in direct contact with the underlying migmatites (Figure 6D), and the basal *Etusis Formation* of the Damara Supergroup is not present. Fabrics in the underlying migmatites are concordant with the fabric in the overlying Khan Formation (Figure 6).

On the eastern limb of the Husabberg Anticlinorium, the Damara metasedimentary Supergroup differs significantly from that defined elsewhere in the southern Central Zone. It consists of a quartz-biotite gneiss unit immediately overlying diatexite migmatites in the dome core, overlain by a ~100 metre thick feldspathic quartzite (most similar to the *Etusis Formation* of previous studies). The *Khan*, *Rössing* and *Chuos* formations of the widely accepted Damara Supergroup succession are all missing, and thick marble units most closely resembling the *Karibib Formation* near the top of the Swakop Group outcrops in direct contact with supposedly basal *Etusis Formation* quartzites of the Nosib Group (Figure 12). The stratigraphic succession of the Damara Supergroup is inconsistent throughout the study area.

Figure 10 – Photomontage (looking towards the south) showing a several-hundred-metre-thick sequence of quartz-diopside-epidote-hornblende-biotite gneiss (i.e., "Khan Formation") of the overlying Damara Supergroup outcropping in a synformal structure on the western limb of the Ida Dome. Granite intrusion into these overlying metasedimentary units is restricted to a minor volume of leucogranite dykes.

3.3 Contact between the underlying migmatites and overlying Damara Supergroup

The contact between underlying migmatites in the dome cores and overlying successions of the Damara metasedimentary Supergroup is indistinct and difficult to pinpoint. It is defined by a gradually increasing proportion of intrusive granite over distances of tens to hundreds of metres inwards towards the core of the domes (Figure 11 and 12). The contact is diffuse and cannot be sharply defined at a specific location. A distinct erosional contact or lithostratigraphic boundary is not observed - the overlying metasedimentary units do not cross-cut the underlying granites or migmatites in the study area. Instead, metasedimentary units resembling the Damara Supergroup continue to outcrop as disaggregated rafts and laterally-continuous horizons amongst the migmatites and leucogranites in the cores of both domes (Section 3.1.3). The contact is an intrusive boundary (Figure 11 and 12), defined by the transition from coherent overlying metasedimentary units on dome limbs (Figure 10) to an intrusive melt-dominated architecture at deeper structural levels in dome cores (Figures 4 to 9).

Leucogranite accumulations comprise up to 80% of the outcrop area at the deepest structural level of the Ida Dome (Figure 8), and similar leucogranite dyke networks intrude into the overlying *Khan Formation* of the Damara Supergroup on the dome limbs (Figure 11D). The leucogranites form an interconnected, anastomosing, network which merge seamlessly with one another and do not crosscut each other (Figure 8 and 11).

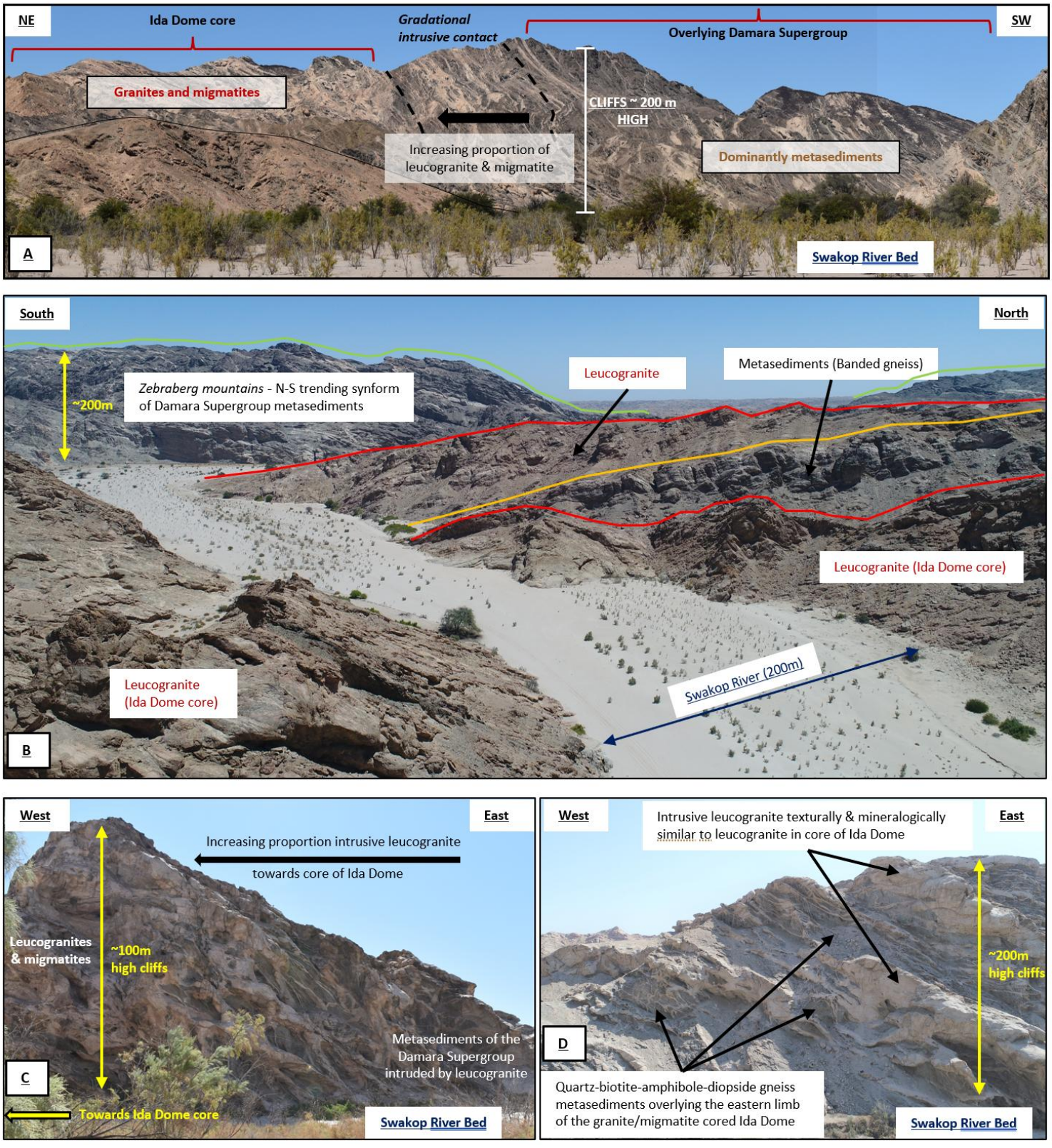

Figure 11 - Contact between granites and migmatites in the core of the Ida Dome with the overlying metasedimentary units of the Damara Supergroup. A) Panoramic photomontage showing the contact on the western limb of the dome. B) Aerial photograph looking outwards from the core of the Ida Dome, showing how leucogranites and migmatites in the dome core are overlain by Damara Supergroup metasediments on the dome limb. C) Photo from the Swakop River showing a gradational contact on the eastern limb of the Ida Dome. D) Metasedimentary units of the Damara Supergroup outcropping in a cliff section on the eastern limb of the Ida Dome. The metasediments are heavily intruded by a leucogranite dyke network.

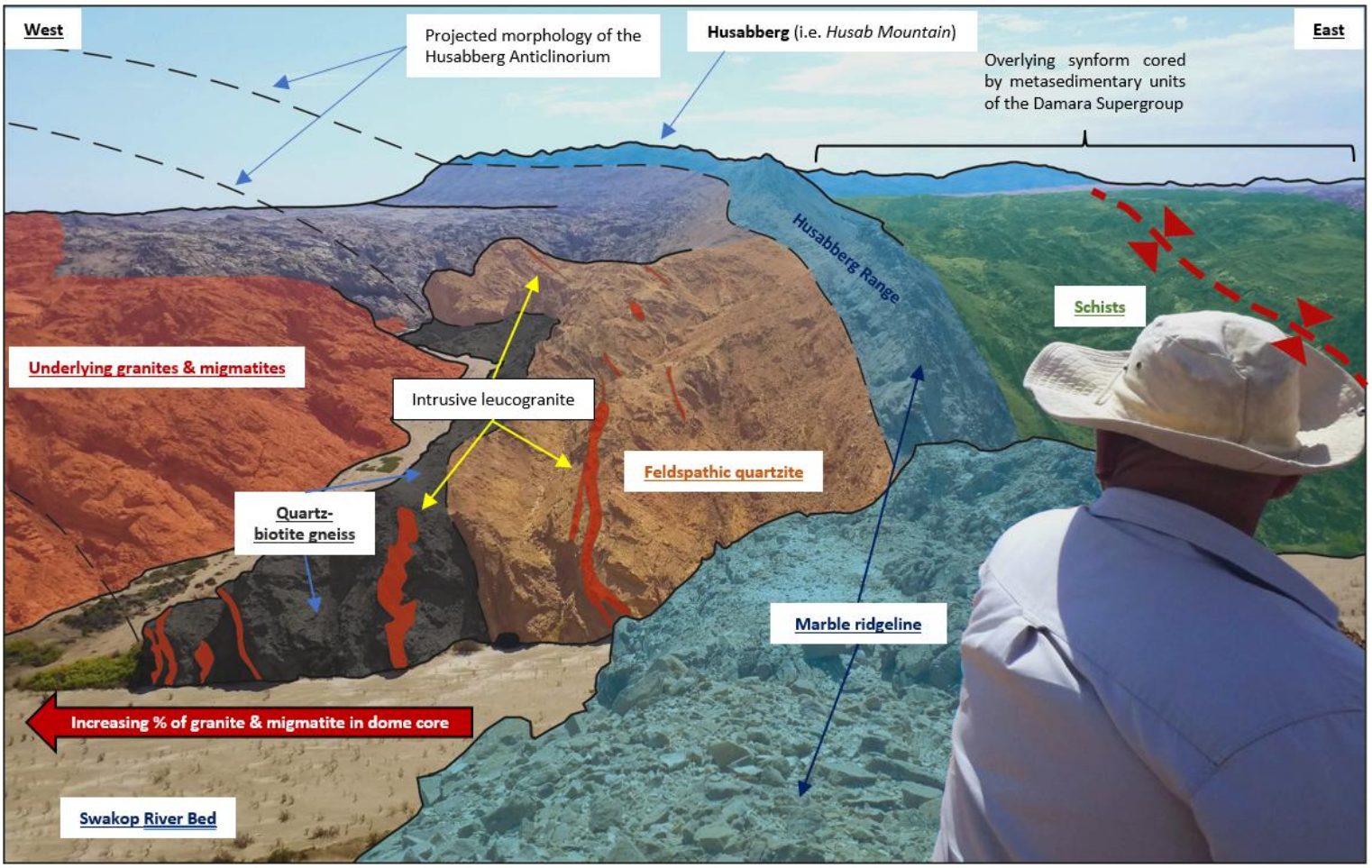

Figure 12 – View towards the north, highlighting how granites and migmatites intrude into and cross-cut the overlying metasedimentary units of the Damara Supergroup on the eastern limb of the Husabberg Anticlinorium.

176
177
178
179
180
181
182
183
184
185
186
187
188

3.4 Geochemical Data

Geochemical sampling includes the following dataset:

- ***Leucogranite dykes***: 12 samples of leucogranite dykes intruding into the *Khan Formation* of the Damara Supergroup on the western, eastern, and southern limbs of the Ida Dome.
- ***Leucosomes from migmatites***: 8 samples of leucosomes from migmatites in the core of the Ida Dome.

3.4.1 Major, trace, and rare earth element behaviour

Leucogranite dykes and leucosomes have similar major element compositions. Both populations have high silica contents; dykes average 74.22% while leucosomes average 74.63%. Leucosomes are slightly more Ca-rich, Fe2O3(t)-rich, and TiO2-rich, while dykes are slightly more K2O-rich (Figure 13A).

Leucogranites and leucosomes have similar overall trends in trace element composition (Figure 13B). They are depleted in Cr and Co and notably enriched in Rb, Ba, Th, and U. While the trend is similar, there are differences in some individual trace element concentrations; leucosomes are more enriched in Sr, Y, Zr, Hf, Ba and Th. Meanwhile, leucogranite dykes are more enriched in Ta, W, and U, and marginally more enriched in Rb, Nb, and Cs.

Leucogranites and leucosomes show very similar trends in REE behaviour (Figure 13C). They are light REE enriched and have a steep negative slope from La to Sm, followed by a flatter profile from Gd to Lu. Both populations have a clear negative Eu anomaly, although this is slightly larger in the dykes than the leucosomes. However, leucogranite dykes are significantly depleted in total REE abundance relative to the leucosomes.

Figure 13 – A) Box and whisker plots of major element oxides by weight % in leucosomes of migmatites vs overlying leucogranite dykes. B) Chondrite-normalised trace element concentrations. Chondrite values from Anders and Grevesse (1989). C) Chondrite-normalised rare earth element (REE).

212

213

214

215

216

3.4.2 Element pair and ratio plots

Specific elements are removed from the melt as minerals crystallise, meaning melt composition evolves along predictable trends. Element pair and ratio plots help to isolate specific mineral control, test closed system fractional crystallisation, and separate fractionation from melting or mixing processes (see Appendix I). Results for dyke and leucosome samples are plotted in Figure 14:

A. ***Ba vs Sr***: Strong positive correlation - dykes have lower Ba and Sr concentrations than the leucosomes.
B. ***Rb/Sr vs Sr***: Strong inverse trend - dykes extend to lower Sr and higher Rb/Sr values than the leucosomes.
C. ***Eu/Eu* vs Sr***: Weak positive correlation - leucosomes generally have higher Sr concentrations and higher Eu/Eu* ratios than most dykes. However, two dykes are outliers with comparatively high Eu/Eu* ratios at low Sr concentrations.
D. ***K/Rb vs Rb***: Strong inverse trend - dykes have higher Rb concentrations and lower K/Rb ratios than the leucosomes.
E. ***Th vs La***: Strong positive correlation – leucosomes and dykes are clustered along a positive trend. Dykes show slightly more scatter than leucosomes and plot at slightly lower La concentrations at given Th concentration. Dykes have lower Th and La concentrations than leucosomes overall.
F. ***Zr vs Hf***: Strong positive linear trend with tight clustering along trend and no deviation. Leucosomes extend to higher Zr and Hf concentrations overall, with dykes dropping to lower concentrations. There is overlap between both populations.
G. ***Th vs Zr***: Dykes and leucosomes show positive correlation along the same trend. Dykes generally plot at lower Th and Zr concentrations than the leucosomes.
H. ***Zr vs Y***: Broad positive correlation overall. Leucosomes occupy higher Zr and Y than dykes, with both populations lying laong the same trend.
I. ***Ta vs Nb***: Strong positive correlation. Leucosomes and dykes are tightly clustered along the same slope. Both populations overlap, but dykes extend to slightly higher Ta and Nb values while leucosomes drop to slightly lower concentrations.
J. ***Nb/Ta vs Nb***: No correlation - the Nb/Ta ratio remains constant at different Nb concentrations.
K. ***Y vs Yb***: Strong positive correlation. All samples plot along a tight linear trend. Both populations overlap, but leucosomes extend to higher Y and Yb concentrations overall while dykes drop to lower absolute values.

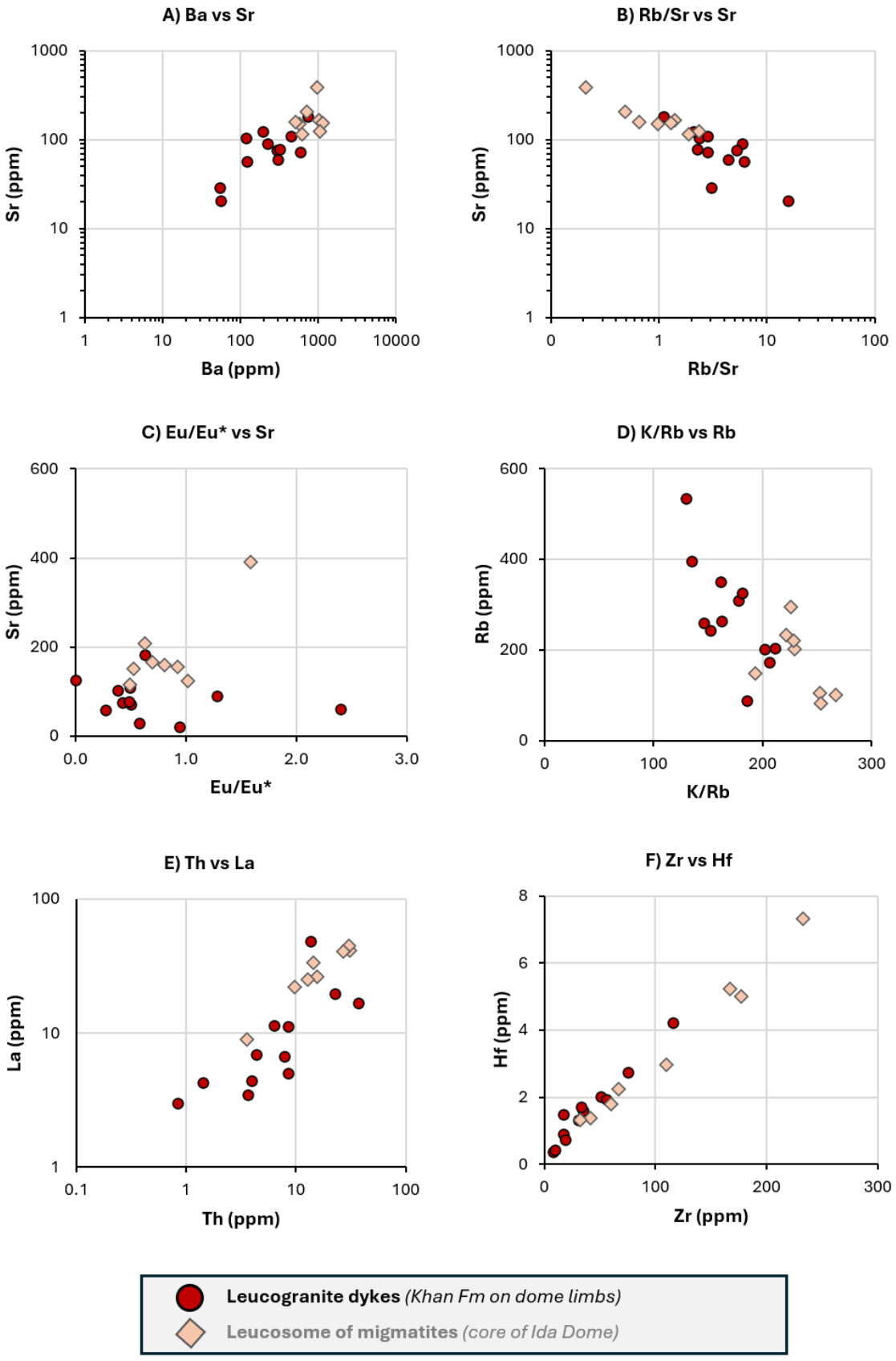
A) Ba vs Sr
Sr (ppm)
Ba (ppm)
B) Rb/Sr vs Sr
Sr (ppm)
Rb/Sr
C) Eu/Eu* vs Sr
Sr (ppm)
Eu/Eu*
D) K/Rb vs Rb
Rb (ppm)
K/Rb
E) Th vs La
La (ppm)
Th (ppm)
F) Zr vs Hf
Hf (ppm)
Zr (ppm)
Leucogranite dykes (Khan Fm on dome limbs)
Leucosome of migmatites (core of Ida Dome)

249

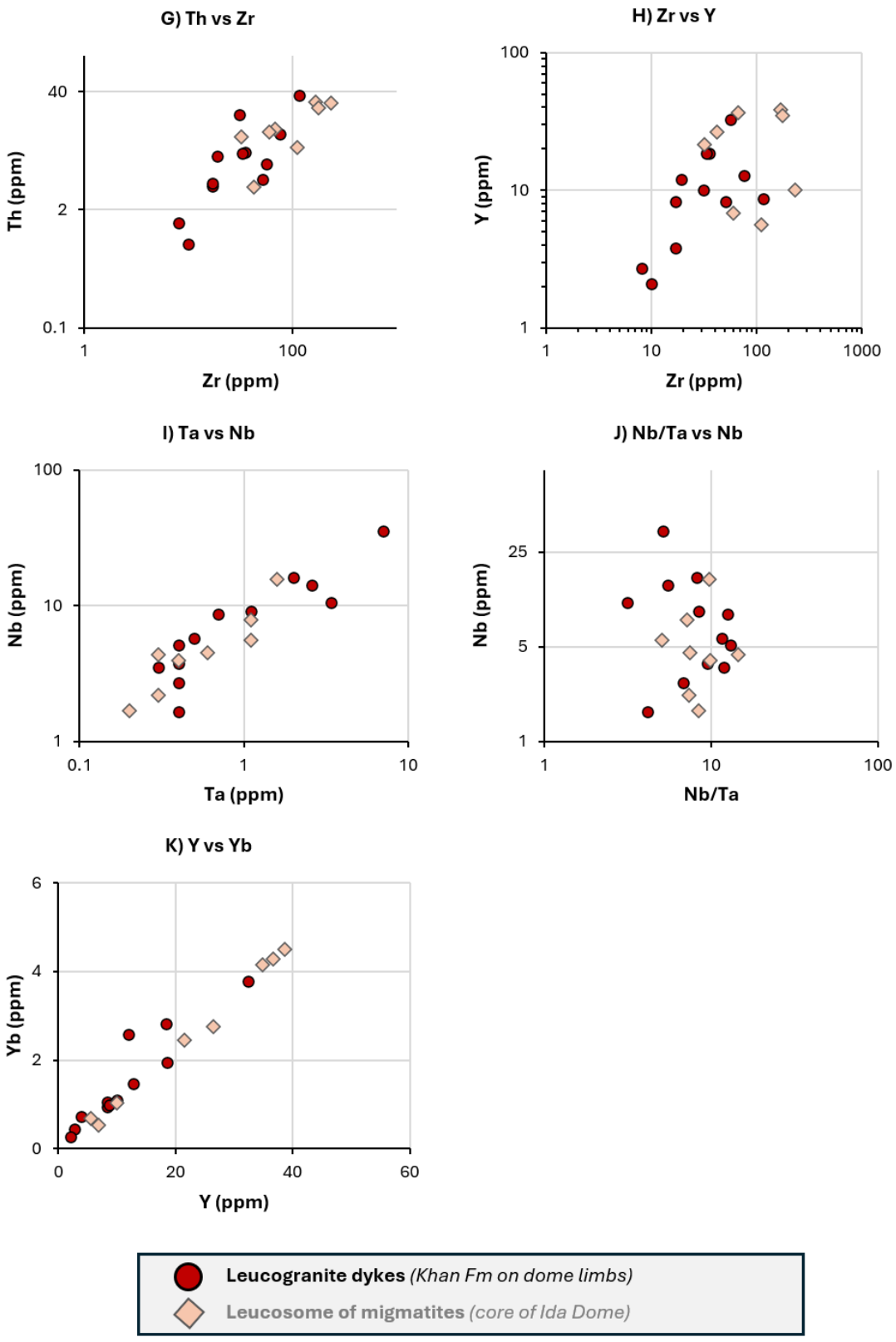

Figure 14 - Element pair and ratio plots for leucogranite dykes and leucosomes of migmatites. A) Ba vs Sr, B) Rb/Sr vs Sr, C) Eu/Eu vs Sr, D) K/Rb vs Rb, E) Th vs La, F) Zr vs Hf, G) Th vs Zr, H) Zr vs Y, I) Ta vs Nb, J) Nb/Ta vs Nb, K) Y vs Yb.*

250

4. DISCUSSION

4.1 A widespread mid-crustal migmatite-granite system / melt-dominated architecture

The core of the Ida Dome and Husabberg Anticlinorium consists overwhelmingly of (1) metatexite and diatexite migmatites (Figures 5 to 7), (2) larger leucogranite dykes, sills and pluton-like accumulations (Figure 8 and 9), and (3) subordinate older country rocks preserved as rafts and schlieren which often have a similar metasedimentary composition to the overlying country rocks of the Damara Supergroup (Section 3.1.3). Underlying granites and migmatites in the dome cores cross-cut the overlying metasedimentary units of the Damara Supergroup along a diffuse and intrusive contact (Figure 11 & 12), constraining a relatively younger age for the underlying migmatites and granites. The overwhelming majority of the outcrop area resembles a mid-crustal migmatite-granite system similar to that mapped and documented in other orogenic belts worldwide (e.g. Brown, 2007, 2013).

4.2 Evidence for differentiation during magma extraction from the migmatite complex and intrusion into overlying metasedimentary units

Field evidence, in the form of petrographic continuity between different melt-bearing structures, suggests that migmatites and leucogranites in the dome cores formed part of a laterally and vertically connected migmatite–granite system which extended throughout the Ida Dome and Husabberg Anticlinorium (Figure 5 to 9), and intruded into overlying Damara metasedimentary units via an interconnected dyke network (Figures 6D, 11 & 12; shown conceptually in Figure 16).

Whole-rock geochemical data provides an independent assessment of magma connectivity between leucosomes in the underlying migmatite complex and leucogranite dykes intruding into the overlying Damara Supergroup. Similar major element compositions, along with near-parallel patterns on trace element spider diagrams, and similar behaviour on REE spider diagrams (Figure 13), supports a close genetic relationship between leucosomes in the migmatites and overlying dyke networks intruding the Damaran metasedimentary units; this is compatible with derivation from a common magmatic system. Dykes and leucosomes fall along near identical trends on element pair and ratio plots (Figure 14), suggesting that similar mineralogical controls and differentiation trends governed both populations. However, the more distal dykes on dome limbs are consistently more evolved than leucosomes in the dome core:

- Dykes have slightly higher K2O contents - consistent with k-feldspar enrichment, along with slightly lower CaO and TiO2 contents - implying plagioclase and biotite/ilmenite/titanite removal, respectively (Figure 13A).
- Dykes have a relatively stronger Eu anomaly (Figure 13C), implying more plagioclase fractionation.
- Dykes fall lower than leucosomes on the Ba vs Sr plot (Figure 14A), consistent with greater plagioclase and K-feldspar removal.
- Dykes have lower Sr and higher Rb/Sr ratios (Figure 14B), again implying more plagioclase fractionation since Rb stays incompatible while Sr is removed in plagioclase.
- Dykes have higher Rb concentrations and lower K/Rb ratios than leucosomes (Figure 14D), again consistent with them being more evolved, since Rb is more incompatible than K and hence concentrates in late melt.

Field and whole rock geochemical data is consistent with extraction and upward migration of leucogranite magma out of the migmatite complex and into more coherent overlying units of the Damara Supergroup. Dykes and leucosomes extend towards opposite ends of element pair and ratio plots while overlapping in the middle (Figure 14). The dykes represent relatively more evolved melt than the underlying leucosomes, suggesting that differentiation occurred during magma extraction and ascent (Figure 16).

4.3 Evolution of the migmatite-granite complex

We propose that the observed migmatite-granite system is consistent with the following conceptual evolution:

1. ***Partial melting, melt migration & melt accumulation***: Local evidence for in-situ partial melting includes coarse garnet megacrysts associated with leucosomes in patch migmatites (Figure 7A). This is consistent with melting reactions reported in nearby country rocks (Ward et al., 2008; Jung et al., 2019). However, the volume of granite present is almost certainly too large for these migmatites to have formed entirely via in-situ partial melting (e.g., Figure 8 & 9). Fabrics and textures are instead consistent with mesoscale melt migration along foliation planes, through cross-cutting shear bands, and along larger dyke-like structures to form larger granite accumulations (Figures 5 to 9). Pervasive mesoscale melt migration in this way is well documented from both the Damara Belt (Kisters et al 2009; Hall and Kisters, 2012, 2016a,b;

Kruger and Kisters, 2016) and other orogenic belts worldwide (Weinberg & Searle, 1998; Weinberg, 1999; Brown, 2007, 2013). Migmatites in the core of the Ida Dome and Husabberg Anticlinorium resemble 'injection migmatites' (e.g., Weinberg & Searle, 1998; Weinberg, 1999).

2. ***Magma front and nature of the contact between migmatites in the dome cores and coherent overlying Damara Supergroup metasediments***: Small volumes of melt can migrate pervasively along foliation planes and through shear bands without freezing if country rock temperatures exceed the melt solidus (Weinberg, 1999; Leitch & Weinberg, 2002; Brown, 2007; Cruden and Weinberg, 2018). This is common in higher-temperature mid- to lower-crustal settings, but colder overlying crustal rocks cause these small bodies of melt to freeze at the 'magma front'. Further granite intrusion above the magma front is typically restricted to dykes, since dykes can propagate faster and transport larger magma bodies which are better insulated against freezing (Cruden and Weinberg, 2018). Field relations indicate that the contact between migmatites in the dome cores and the overlying Damara Supergroup is intrusive and indistinct (Section 3.3; Figure 11 & 12). Below this boundary, melt is pervasively distributed in small (cm-scale) bodies arranged along foliation planes, in boudin necks, and in small-scale shear bands (Figure 5 to 9). Above this contact, granite intrusion is limited mostly to larger (metre-scale) anastomosing dyke networks which cross-cut coherent metasedimentary units of the Damara Supergroup (Figure 11 & 12). The geometry and morphology of this contact is consistent with the location of the 'magma front' (Figure 16). Leitch and Weinberg (2002) demonstrated that the position of a magma front is not fixed in space or time, since pervasive magma intrusion can locally increase the temperature of country rocks via heat advection; this allows the magma front to push higher into overlying rocks. The height of the magma front relative to the country rock stratigraphy may therefore vary spatially from one dome structure to another. This can explain both the absence of the *Etusis Formation* at the Arcadia Synform (Figure 6D), and why the metasedimentary succession overlying the eastern limb of the Husabberg Anticlirnorium differs from that described for the Damara Supergroup elsewhere in the southern Central Zone (Section 3.2); since the magma front is a temperature-controlled boundary, it need not be confined to a distinct lithostratigraphic horizon (Figure 16).
3. ***Metamorphic conditions and driving force***: Regional temperatures reached ~800^{O}C throughout the southwestern Central Zone during later stages of the Damara Orogeny; this was contemporaneous with widespread leucogranite magmatism at c. 520 Ma (Longridge et al., 2017; Jung et al., 2019; MacRoberts et al., 2025). This provides the necessary conditions and driving force for formation of the observed migmatite-granite complex.

4.4 Protolith rocks to the migmatites: Circa 1-2 Ga pre-Damaran Abbabis Complex basement or deeper levels of the ca. 870-590 Ma Damara Supergroup?

Migmatites and granites comprise up to 80% the of the outcrop area in the core of the Ida Dome and Husabberg Anticinorium, with the remaining 20% consisting of subordinate country rock rafts (Figure 5 to 9). Since the migmatites and granites intrude into and cross-cut the overlying ca. 870-590 Ma metasedimentary units of the Damara Supergroup along an intrusive contact (e.g., Figure 11 and 12), much of the outcrop area in the Ida Dome and Husabberg Anticlinorium consists of Damaran-aged igneous material (Figure 5 to 9). The age and nature of the country rock protoliths to these migmatites remains equivocal.

Published CL imaging and U–Pb datasets from the Abbabis Complex basement in the southern Central Zone reveals a population of oscillatory-zoned, euhedral to subhedral zircons with ages clustering around ~1 and 2 Ga (Figure 15; Jacob et al., 1978; Kroner et al., 1991; Tack et al., 2002; Longridge, 2012; Foster et al., 2015; Longridge et al., 2018; Goslin, 2019). However, similarly aged ca. 1-2 Ga detrital zircon xenocrysts also exist in the lower Khan and Etusis formations of the Damara Supergroup (Figure 15), meaning these units cannot be easily distinguished from zircon ages alone. Since metasedimentary units outcropping as disaggregated rafts and laterally continuous horizons amongst the granites and migmatites in core of the Ida Dome and Husabberg Anticlinorium superficially resemble those of the overlying Damara Supergroup (Barnes, 1981; this study Section 3.1.3), it is extremely difficult to distinguish whether the protolith country rocks represent either ca. 1-2 Ga pre-Damaran Abbabis Complex basement, or deeper structural levels of the ca. 870-590 Ma Damara Supergroup. We limit our findings to the observation that the dominant rock volume in the core of the Ida Dome and Husabberg Anticlinorium consists of a widespread migmatite-granite system formed via syn-orogenic magmatism during granulite facies metamorphism at c. 530-510 Ma in the Damara Orogeny (Figure 5-9; Figure 16). The nature of the protolith country rocks remains equivocal.

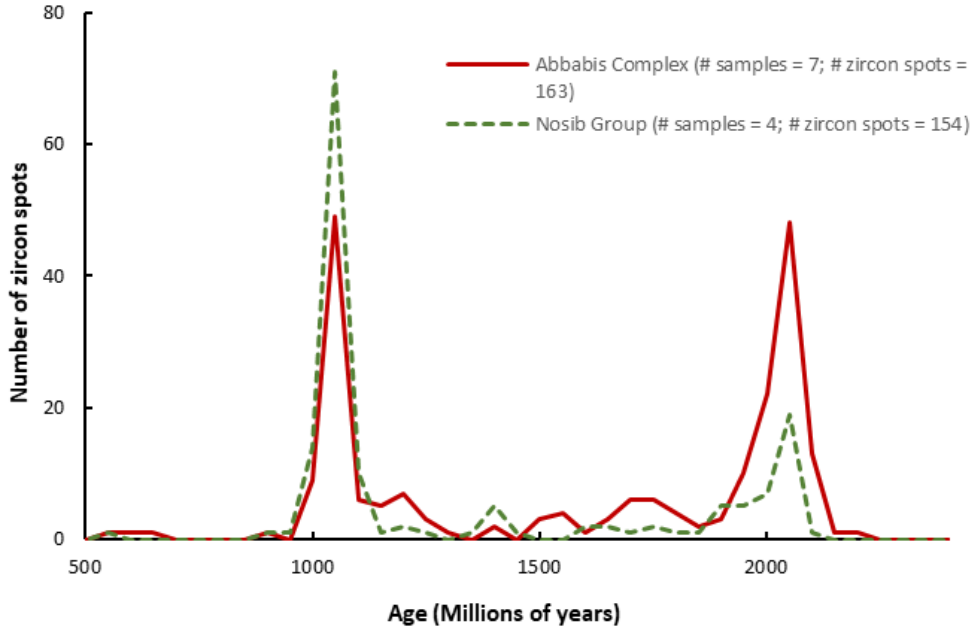

Figure 15 – Compilation of existing U-Pb zircon age data for the Abbabis Complex and the Nosib Group (Khan & Etusis Formations) of the Damara Supergroup. Data sources: Kroner et al., 1991; Foster et al., 2015; Longridge et al., 2018; Goslin, 2019.

4.5 Implications of the melt-dominated architecture on the physical state, rheology and deformation mechanisms within the mid-crust of the Damara Orogen

The geology of the study area has a layered mid-crustal architecture as shown in Figure 16. Thicker and more coherent overlying metasedimentary units are underlain by an extensive migmatite-granite domain in the dome cores which represents the extent of formerly partially molten crust (Figure 5-9). Broadly similar findings have been reported from the Khan/Palmenhorst Dome immediately west of our study area (Toe et al., 2013), indicating that this melt-dominated domain was likely widespread.

Experimental and theoretical studies show that modest melt fractions <10% can dramatically reduce the strength of rocks by up to 90%, causing significant reductions in the viscosity of the crust (Rosenberg and Handy, 2005; Jamieson et al., 2011). The partially-molten domain (>80% leucogranite/migmatite; Figure 16) documented in the core of the Ida Dome and Husabberg Anticlinorium in this study provides the geological basis for a broader discussion of deformation mechanisms and tectonic style in the mid-crust of the Damara Orogen, including a potential transition from localised strain accumulation to distributed ductile flow (e.g., Jamieson et al., 2011; Jamieson and Beaumont, 2013). Peak granulite-facies metamorphic conditions of ~800 °C and 4–5 kbar coincided with widespread leucogranite generation between ca. 530–510 Ma (Longridge et al., 2017; Jung et al., 2019; MacRoberts et al., 2025), implying that the partially molten crust may have persisted for tens of millions of years. This is discussed in two companion paper which present a new structural field dataset (Jones, 2026), along with new orogen-scale structural mapping and belt-scale synthesis of lithostratigraphic, metamorphic, magmatic, and geochronological data (Jones et al., 2026). The melt-dominated architecture in the core of the Ida Dome and Husabberg Anticlinorium (Figure 16) also has strong relevance for understanding the evolution of world-class uranium mineral deposits hosted in intrusive leucogranite dykes on dome limbs (Kinnaird and Nex, 2007).

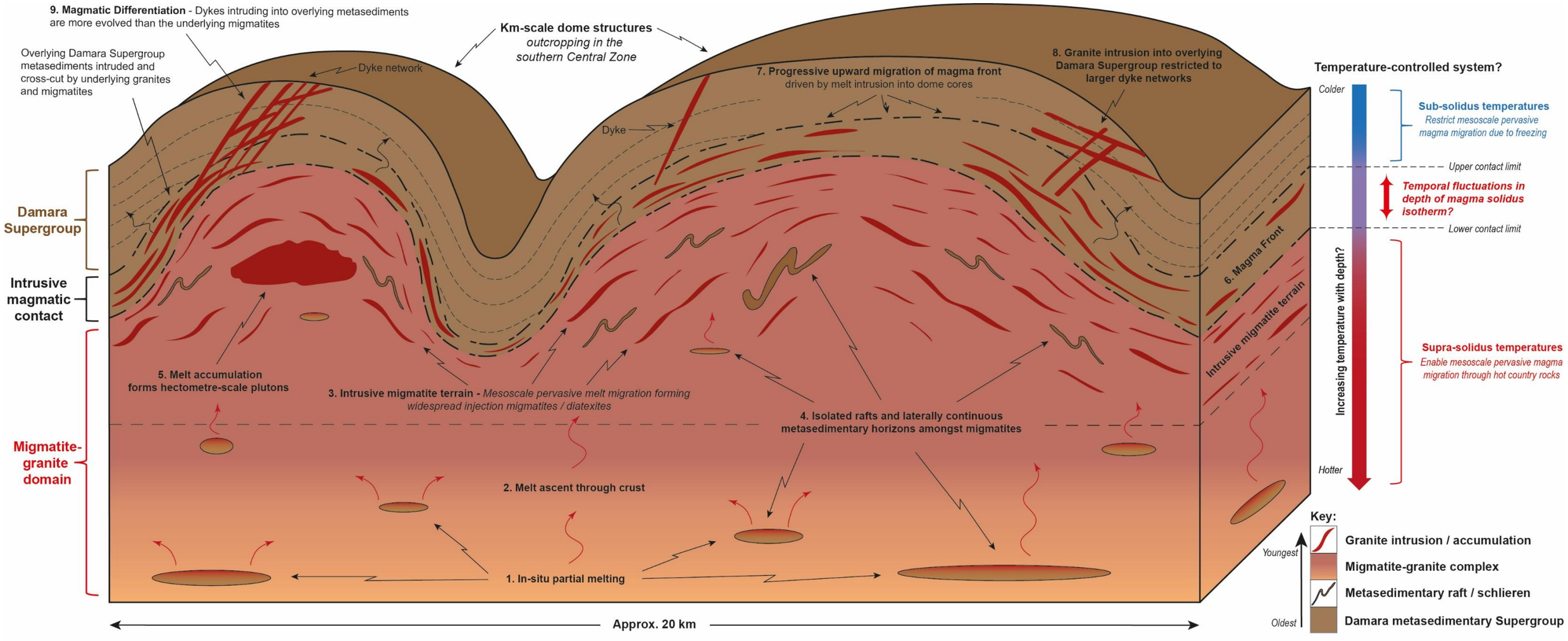

'Mesoscale pervasive flow' - Term used to describe the pervasive migration of small batches of magma (typically cm-scale) through an extensive network of channels, such as along foliation planes, through shear bands, or fold axial planes. Concept arises from field studies of migmatite terrains and contrasts with magma transport via dyking (although both dykes and pervasive flow may coexist).

'Magma Front' - Shallowest depth at which magma can migrate by mesoscale pervasive flow. Likely corresponds to depth of the magma solidus - at shallower depths, colder rocks cause the magma to freeze, which prevents small batches of melt from migrating pervasively along foliation planes and shear bands (Leitch & Weinberg, 2002)

Figure 16 – Conceptual model for the formation and evolution of a mid-crustal migmatite-granite network as observed in the Ida Dome and Husabberg Anticlinorium. Upward migration of melt through the domes is associated with magmatic differentiation; dykes intruding into the overlying Damara Supergroup are relatively more evolved than the migmatitic leucosomes in the dome cores..

5. Conclusions

Field relationships, remote sensing observations, and whole-rock geochemistry from the Ida Dome and Husabberg Anticlinorium document the existence of an interconnected syn-orogenic migmatite–granite domain in the former mid-crust of the Damara Orogen. Coherent metasedimentary packages on dome limbs become progressively invaded by an increasing proportion of leucogranite and migmatite inwards towards dome interiors, producing a diffuse transition from metasediment-dominated to melt-dominated crust. The melt-dominated architecture is dominated by metatexite and diatexite migmatites, interconnected leucogranite sheets and dykes, plus entrained and disaggregated metasedimentary rafts and schlieren compositionally similar to the overlying Damara Supergroup. Petrographic continuity, together with closely overlapping major- and trace-element compositions and shared fractionation trends, are consistent with an interconnected melt-transfer system accommodating melt ascent from underlying migmatites in the dome cores upwards into voluminous leucogranite dyke networks which intrude the overlying Damara metasedimentary Supergroup. Overlying dykes have more evolved geochemical signatures, consistent with progressive differentiation during magma ascent. The migmatite-granite system is volumetrically dominant in the cores of the Ida Dome and Husabberg Anticlinorium (>80% of outcrop area, plus ~20% older country rock rafts) and is likely to have impacted the rheology of the crust, reducing viscosity and potentially providing the conditions necessary for a transition from localised strain accumulation to more distributed ductile deformation.

6. ACKNOWLEDGMENTS

This work was undertaken as part of T. Jones' PhD research. The support of the DST-NRF Centre of Excellence for Integrated Mineral and Energy Resource Analysis (DST-NRF CIMERA) towards this research is hereby acknowledged. Additional support provided by the Society of Economic Geologists (SEG) in the form of a Graduate Student Fellowship and a Student Research Grant from the McKinstry Fund is greatly appreciated. Deep Yellow Ltd contributed towards the PhD funding of T. Jones and provided logistical support during fieldwork. Judith Kinnaird, Paul Nex and Roger Gibson are thanked for extensive discussion on this topic and earlier versions of the manuscript prior to submission. Opinions expressed and conclusions arrived at are solely those of the authors; they do not represent the opinions or conclusions of the supporting bodies or acknowledged individuals.

Appendix I : Description of element pair and ratio plots

Feldspar fractionation:

- ***Ba vs Sr*** plots track feldspar control on the system, since Ba is mostly partitioned into K-feldspar while Sr is partitioned into plagioclase.
- ***Rb/Sr vs Sr*** plots primarily track plagioclase control. Plagioclase crystallisation removes Sr, whereas Rb is highly incompatible and remains in the melt.
- ***Eu/Eu* vs Sr*** further tests plagioclase control. Both Eu and Sr substitute into plagioclase, meaning that Sr and Eu/Eu* typically produce a positive correlation as plagioclase crystallises.

Degree of differentiation:

- ***K/Rb vs Rb*** tests the degree of differentiation. Like K, Rb substitutes into K-feldspar and biotite. However, Rb is more incompatible than K, meaning that it is removed from the melt less efficiently. Differentiation therefore results in higher Rb concentrations and lower K/Rb ratios.

Accessory mineral control:

- ***Th vs La*** typically tracks accessory mineral control – especially monazite. Monazite crystallisation removes Th and LREE (for which La is a proxy) from the melt.
- ***Zr vs Hf*** tracks zircon. Since Zr and Hf are geochemical twins, they substitute into zircon near-identically. Under closed-system differentiation they maintain a near-constant ratio. Deviations imply different source signatures, inheritance, accumulation, contamination or different melt populations. Higher Zr-Hf values in a sample can reflect entrained/inherited zircon crystals, hotter melts which dissolved more zircon (zircon solubility in melt is strongly temperature dependent), or zircon crystallisation.
- ***Th vs Zr*** tracks the relationship between accessory phases monazite (Th control) and zircon (Zr control). Tight linear correlation suggests accessory phases behaved coherently, while scatter or decoupling can imply independent fractionation, different melting reactions, or source heterogeneity.
- ***Zr vs Y*** tests zircon behaviour against accessory minerals controlling HREE/Y-bearing phases. Y can be affected by retained garnet in the source, as well as xenotime and monazite.
- ***Ta vs Nb*** tracks high field strength element (HFSE) behaviour. Nb and Ta are geochemical twins which behave similarly and are mostly controlled by accessory phases such as rutile, ilmenite and titanite, as well as residual phases in the source.

- ***Nb/Ta vs Nb*** tests whether the Nb/Ta ratio changes as the system becomes more enriched in Nb. Changes in Nb/Ta ratio with Nb enrichment can indicate Ti-phase fractionation, source heterogeneity, or mixing between melts with different Nb/Ta ratios. Conversely, coherent behaviour implies no strong fractionation between Nb and Ta, no obvious rutile-controlled residual effect, and likely a similar source reservoir.
- ***Y vs Yb*** tracks HREE behaviour, and is often a check on garnet, xenotime and amphibole control. Tight positive linear trends indicate that HREEs are behaving coherently, with differences between populations mostly due to degree of enrichment or dilution rather than residual mineralogy. Decoupling, scatter, or multiple trends can conversely indicate garnet in the residue, xenotime or monazite affects, or mixing between melts.

7. REFERENCES CITED

Anders, E., Grevesse, N., 1989. Abundances of the elements: meteoric and solar. *Geochim. Cosmochim. Acta* **53**, 197–214.

Ashworth, L., Kinnaird, J.A., Nex, P.A.M., Harris, C., Müller, A., 2020. Origin of rare- element-mineralized Damara Belt pegmatites: a geochemical and light stable isotope study. *Lithos* **372–373**, 105655. https://doi.org/10.1016/j.lithos.2020.105655. ISSN: 0024-4937.

Barnes, J.F.H. and Downing, K.N. 1979. Origin of domes in the central Damara belt, Namibia. *Rev. Geol. Dynam. Geogr. Phys. 21, 383-386*.

Barnes, J.F.H., 1981. Some aspects of the tectonic history of the Khan-Swakop region of the Damara Belt, Namibia. *Unpublished PhD thesis, University of Leeds, United Kingdom*.

Brown, M., 2007.Crustal melting and melt extraction, ascent and emplacement in orogens: Mechanisms and consequences. *Journal of the Geological Society* **164**, 709–730.

Brown, M., 2013. Granite: From genesis to emplacement. *Bulletin of the Geological Society of America* **125**, 1079–1113.

Cruden, A.R., Weinberg, R.G., 2018. Mechanisms of magma transport and storage in the lower and middle crust—magma segregation, ascent and emplacement. In: Burchardt (Ed.), Volcanic and Igneous Plumbing Systems Understanding Magma Transport, Storage, and Evolution in the Earth's Crust. *Elsevier*, pp. 13–53.

Foster, D.A., Goscombe, B.D., Newstead, B., Mapani, B., Mueller, P.A., Gregory, L.C., Muvangua, E., 2015, U-Pb age and Lu-Hf isotopic data of detrital zircons from the Neoproterozoic Damara Sequence: Implications for Congo and Kalahari before Gondwana, *Gondwana Research*, **28 (1)**, 179-190

Geological survey of Namibia 1995. Map Sheet 2214: Walvis Bay. *Geological Survey of Namibia, Windhoek*.

Goscombe, B., Foster, D. A., Gray, D., & Wade, B. 2017. Metamorphic response and crustal architecture in a classical collisional orogen: The Damara Belt, Namibia. *Gondwana Research*, **52**, 80– 124. https://doi.org/10.1016/j.gr.2017.07.006

Goslin, L.M., 2019. Deformation and partial melting in the Central Zone of the Damara Orogen, Namibia. *Unpublished Ph.D. thesis, University of the Witwatersrand*.

Hall, D. and Kisters, A., 2012. The stabilization of self-organised leucogranite networks-Implications for melt segregation and far-field melt transfer in the continental crust. *Earth and Planetary Science Letters*, 355-356: 1-12.

Hall, D., & Kisters, A. (2016a). From steep feeders to tabular plutons—emplacement controls of syntectonic granitoid plutons of the Damara Belt, Namibia. Journal of African Earth Sciences, 113, 51–64. https://doi.org/10.1016/j.jafrearsci.2015.10.005

Hall, D., and Kisters, A., 2016b, Episodic granite accumulation and extraction from the mid-crust: Journal of Metamorphic Geology, v. 34, p. 483–500, https://doi.org/10.1111/jmg .12190.

Hoffmann, K.-H., Condon, D. J., Bowring, S.A.& Crowley, J. L. 2004. U–Pb date from the Neoproterozoic Ghaub Formation, Namibia: Constraints on Marinoan glaciation. *Geology*, **29**, 1091–1094.

Jacob, R.E., 1974. Geology and metamorphic petrology of part of the Damara orogen along the lower Swakop river, South West Africa. *Unpublished PhD thesis, University of Cape Town, South Africa*.

Jacob, R.E., Kröner, A. and Burger, A.J., 1978. Areal extent and first U-Pb age of the Pre-Damaran Abbabis complex in the central Damara belt of South West Africa (Namibia). *International Journal of Earth Sciences*, **67**, 706–718.

Jacob, R.E., Snowden, P.A., Bunting, F.J.L., 1983. Geology and Structural development of the Tumas basement dome and its cover rocks. In: Miller, R.McG. (Ed.), Evolution of the Damara Oroqen of South West Africa/Namibia. *Geological Society of South Africa, Special Publication* **11**, pp. 409-421.

Jamieson, R.A., Unsworth, M.J., Harris, N.B.W., Rosenberg, C.L. & Schulmann, K. 2011. Crustal melting and the flow of mountains. *Elements*, **7**, 253–260.

Jamieson, R. A., and C. Beaumont (2013), On the origin of orogens, *Geological Society of America Bulletin*. **125 (11-12)**, 1671–1702

Jones, T.L. 2026. Structural setting of U-bearing pegmatite mineralisation in the Damara Orogen, Namibia. *Ore Geology Reviews – manuscript in review - preprint at*: https://doi.org/10.13140/RG.2.2.34493.52961

Jones, T.L., Knupp, K.P., Otto, A., Becker, E. Wilde, A. 2026. Hot orogen behavior, partial melting and ductile flow: Case study of the Damara Orogen, Namibia. *Tectonics – manuscript in review - preprint at EarthArXiv*: https://doi.org/10.31223/X5VV2J

Jung, S., Brandt, S., Bast, R., Scherer, E.E., Berndt, J., 2019. Metamorphic petrology of a high-T/low-P granulite terrane (Damara belt, Namibia) – constraints from pseudosection modelling and high-precision Lu-Hf garnet-whole rock dating. *Journal of Metamorphic Geology*. **37 (1)**, 41–69. https://doi.org/10.1111/jmg.2019.37.issue- 110.1111/jmg.12448.

Jung, S., Hoernes, S., Mezger, K., 2001. Trace element and isotopic (Sr, Nd, Pb, O) arguments for a mid-crustal origin of Pan-African garnet-bearing S-type granites from the Damara orogen (Namibia). *Precambrian Research*. **110 (1)**, 325–355. https://doi. org/10.1016/S0301-9268(01)00175-9.

Kinnaird, J.A., Nex, P.A.M., 2007. A review of geological controls on uranium mineralisation in sheeted leucogranites within the Damara Orogen, Namibia. *Trans I.M.M. Applied Earth Sciences* **116(2)**, 68-85.

Kisters, A.F.M., Jordaan, L.S., Neumaier, K., 2004. Thrust-related dome structures in the Karibib district and the origin of orthogonal fabric domains in the south Central Zone of the Pan-African Damara belt, Namibia. *Precambrian Research 133, 283-303.*

Kisters, A.F.M., Ward, R.A., Anthonissen, C.J., Vietze, M.E., 2009, Melt segregation and far-field melt transfer in the mid-crust, *Journal of the Geological Society*, **166 (5)**, 905-918

Knupp, K.P. 2019. Regional Airborne Geophysical Interpretation, Uranium Province, Western Namibia. *Internal report produced on behalf of Reptile Mineral Resources, Swakopmund, Namibia*.

Kroner, A. 1984, Dome structures and basement reactivation in the Pan-African Damara belt of Namibia, in Precambrian Tectonics Illustrated, edited by A. Kroner and R. Greiling, pp. 191 – 206, *E. Schweizerbart'sche, Stuttgart, Germany*.

Kroner, A., Retief, E. A., Compston, W., Jacob, R. E. & Burger, A. J. 1991. Single-grain and conventional zircon dating of remobilized basement gneisses in the central Damara belt of Namibia. *South African Journal of Geology*, **94**, 379-387.

Kruger, T., Kisters, A., 2016. Magma accumulation and segregation during regional-scale folding: the Holland's dome granite injection complex, Damara belt, Namibia. *Journal of Structural Geology* http://dx.doi.org/10.1016/j.jsg.2016.05.002.

Leitch, A.M., and Weinberg, R.F., 2002, Modelling granite migration by mesoscale pervasive flow: *Earth and Planetary Science Letters*, v. **200**, p. 131–146, doi:10.1016 /S0012-821X(02)00596-4.

Longridge, L., 2012. Tectonothermal Evolution of the Southwestern Central Zone, Damara Belt, Namibia. *Unpublished Ph.D. thesis, University of the Witwatersrand, South Africa* (522 pp.).

Longridge, L., Gibson, R.L., Kinnaird, J.A. and Armstrong, R.A., 2017. New constraints on the age and conditions of LPHT metamorphism in the southwestern Central Zone of the Damara Belt, Namibia and implications for tectonic setting. *Lithos* , 278-281, 361–382. doi: 10.1016/j.lithos.2017.02.006

Longridge, L., Kinnaird, J.A., Gibson, R., Hawkesworth, C., Armstrong, R., 2018. Crystal recycling in the Damara Belt, Namibia, and interaction of the Congo and KalahariCratons–evidence from zircon U–Pb, Hf and O isotopes. *South African Journal of Geology*. **121 (3)**,237–252.

MacRoberts, R.J. 2025. Polyphase deformation during prolonged high-temperature, low-pressure metamorphism: An example from the Namibfontein-Vergenoeg migmatite domes, Central Zone, Damara Belt, Namibia. *Journal of Metamorphic Geology*. **0**. 1-35.

Miller R. McG., 2008. The geology of Namibia, Vol. 2: Neoproterozoic to Lower Paleocene. *Geol. Survey Namibia, Windhoek. Namibia*.

Miller, R. McG. & Grote, W. 1988. Geological Map of the Damara orogen, Namibia (scale 1:500,000). *Geological Survey of Namibia, Windhoek*.

Oliver, G.J.H., 1994. Mid-crustal detachment and domes in the central zone of the Damara orogen Namibia. *Journal of African Earth Sciences* **19**, 331–344.

Oliver, G.J. 1995. The Central zone of the Damara orogen, Namibia, as a deep metamorphic core complex. *Communications of the Geological Survey of Namibia*, **10**, 33-41.

Ormond, R. J., J. Lehmann, P. Hasalová, and M. Elburg. 2024. Migmatite Dome as a Result of Multi-Fold Interference Pattern, in the Damara Belt, Namibia. *Journal of Structural Geology 180: 105059.*

Paul, A., S. Jung, R. L. Romer, A. Stracke, and F. Hauff (2014), Petrogenesis of synorogenic high-temperature leucogranites (Damara orogen, Namibia): Constraints from U–Pb monazite ages and Nd, Sr and Pb isotopes, *Gondwana Research*, **25(4)**, 1614–1626, doi:10.1016/j.gr.2013.06.008.

Poli, L.C., Oliver, G.J.H., 2001. Constrictional deformation in the Central Zone of the Damara Orogen Namibia. *Journal of African Earth Science*. 33, 303–312.

Rosenberg, C.L., Handy, M.R., 2005. Experimental deformation of partially melted granite revisited: implications for the continental crust. *Journal of Metamorphic Geology*. **23**, 19–28.

Smith, D.A.M., 1965. The geology of the area around the Khan and Swakop Rivers in SW Africa. *Geological Survey South Africa, Memoir 3*, 1-113.

Tack, L., Williams, I. and Bowden, P., 2002. SHRIMP constraints on early post-collisional granitoids of the Ida Dome, central Damara (Pan-African) Belt, western Namibia. *Abstracts of the 11th IAGOD Quadrennial Symposium and Geocongress, Windhoek, Namibia*.

Toé, W., Vanderhaeghe, O., André-Mayer, A.-S., Feybesse, J.-L., & Milési, J.-P. (2013). From migmatites to granites in the Pan-African Damara orogenic belt, Namibia. *Journal of African Earth Sciences*, **85**, 62–74. https://doi.org/10.1016/j.jafrearsci.2013.04.009

Ward R., Stevens G., Kisters A., 2008, Fluid and deformation induced partial melting and melt volumes in low-temperature granulite-facies metasediments, Damara Belt, Namibia: *Lithos* , v. **105**, p. 253–271, doi:10.1016/j.lithos.2008.04.001.

Weinberg, R.F., 1999, Mesoscale pervasive melt migration: Alternative to dyking: *Lithos*, v. **46**, p. 393–410, doi: 10.1016/S0024-4937(98)00075-9.

Weinberg, R.F., and Searle, M.P., 1998, The Pangong injection complex, Indian Karakoram: A case of pervasive granite flow through hot viscous crust: *Journal of the Geological Society of London*, v. **155**, p. 883–891, doi:10.1144/gsjgs.155.5.0883.